American Heart Association | American Stroke Association

Small-Conductance Calcium-Activated Potassium Current in Normal Rabbit Cardiac Purkinje Cells

Thomas A. Reher, MD;* Zhuo Wang, MD;* Chia-Hsiang Hsueh, PhD; Po-Cheng Chang, MD; Zhenwei Pan, PhD; Mohineesh Kumar, MD; Jheel Patel, BS; Jian Tan, MS; Changyu Shen, PhD; Zhenhui Chen, PhD; Michael C. Fishbein, MD; Michael Rubart, MD; Penelope Boyden, PhD; Peng-Sheng Chen, MD

***Background*—**Purkinje cells (PCs) are important in cardiac arrhythmogenesis. Whether small-conductance calcium-activated potassium (SK) channels are present in PCs remains unclear. We tested the hypotheses that subtype 2 SK (SK2) channel proteins and apamin-sensitive SK currents are abundantly present in PCs.

***Methods and Results*—**We studied 25 normal rabbit ventricles, including 13 patch-clamp studies, 4 for Western blotting, and 8 for immunohistochemical staining. Transmembrane action potentials were recorded in current-clamp mode using the perforated-patch technique. For PCs, the apamin (100 nmol/L) significantly prolonged action potential duration measured to 80% repolarization by an average of 10.4 ms (95% CI, 0.11–20.72) (n=9, *P*=0.047). Voltage-clamp study showed that apamin-sensitive SK current density was significantly larger in PCs compared with ventricular myocytes at potentials ≥0 mV. Western blotting of SK2 expression showed that the SK2 protein expression in the midmyocardium was 58% (*P*=0.028) and the epicardium was 50% (*P*=0.018) of that in the pseudotendons. Immunostaining of SK2 protein showed that PCs stained stronger than ventricular myocytes. Confocal microscope study showed SK2 protein was distributed to the periphery of the PCs.

***Conclusions*—**SK2 proteins are more abundantly present in the PCs than in the ventricular myocytes of normal rabbit ventricles. Apamin-sensitive SK current is important in ventricular repolarization of normal PCs. **(*J Am Heart Assoc*. 2017;6:e005471. DOI: 10.1161/JAHA.117.005471.)**

Key Words: action potential • apamin • potassium channels • repolarization

Small-conductance calcium-activated potassium (SK) channels were first cloned in 1996 from neural tissues of the central nervous system.[1] SK channels are sensitive to intracellular calcium but not to membrane potential.[1,2] In the presence of increased intracellular calcium, neuronal SK channels open, causing a flow of intracellular potassium to the extracellular space and hyperpolarizing membrane potential, leading to a slow afterhyperpolarization, which terminates or reduces nerve activity. Apamin, a Western honey bee toxin that specifically inhibits SK channels,[3] reduces the slow afterhyperpolarization and depolarizes the membrane potential, resulting in rapid and irregular neuronal firing.[4] Subsequent studies showed that both SK channel proteins and apamin-sensitive SK currents (I_{KAS}) are abundantly present in the atria, atrioventricular node, pulmonary vein, and ventricular myocytes (VMs) of different species and play an important role in repolarization and arrhythmogenesis especially in heart failure and myocardial ischemia.[5,6] In both normal and failing ventricles, prolongation of the pacing cycle length (PCL) further increases the importance of I_{KAS} in repolarization.[7,8] However, the importance of I_{KAS} in the His-Purkinje system remains unclear. Purkinje cells (PCs) in humans, dogs, and rabbits are found in the subendocardium and in free-running pseudotendons. The availability of repolarization currents is important in subsequent depolarization and rapid conduction through the His-Purkinje system. In addition to conduction, PCs are also important in the initiation and maintenance of ventricular arrhythmias.[9,10] PCs have an increased intracellular calcium-membrane potential coupling

From the Krannert Institute of Cardiology and Division of Cardiology, Department of Medicine, Indianapolis, IN (T.A.R., Z.W., C.-H.H., P.-C.C., Z.P., M.K., J.P., J.T., Z.C., P.-S.C.); Department of Cardiology, Renmin Hospital of Wuhan University, Wuhan, China (Z.W.); Smith Center for Outcomes Research in Cardiology, Beth Israel Deaconess Medical Center, Harvard Medical School, Boston, MA (C.S.); Department of Pathology and Laboratory Medicine, UCLA Medical Center, Los Angeles, CA (M.C.F.); Department of Pediatrics, Indiana University School of Medicine, Indianapolis, IN (M.R.); Department of Pharmacology, Columbia University, New York, NY (P.B.).

*Dr Reher and Dr Wang contributed equally to this study.

Correspondence to: Peng-Sheng Chen, MD, 1800 North Capitol Avenue, E475, Indianapolis, IN 46202. E-mail: chenpp@iu.edu

Received January 2, 2017; accepted February 17, 2017.

gain and are sources of afterdepolarization and triggered activity in rabbit ventricles.[11] PCs can be a source of continuous electrical activity during ventricular fibrillation[12] and are also important in initiating ventricular arrhythmias in humans.[13] High incidence of Ca^{2+} transient wavelets/waves in diseased PCs are responsible for arrhythmias originating in the subendocardial Purkinje network postmyocardial infarction.[14] Because PCs are important in cardiac conduction and arrhythmogenesis, a better understanding of the ionic currents in the PCs is important in managing arrhythmias originated from the PCs. If I_{KAS} contributes to the repolarization of the PCs, then the presence of I_{KAS} may help maintain repolarization reserve and thus is protective against arrhythmias. Drugs that block I_{KAS} may be proarrhythmic by removing the repolarization reserve. On the other hand, an excessive amount of I_{KAS} may shorten the action potential duration (APD) and promote recurrent ventricular fibrillation.[15] Therefore, I_{KAS} blockade may be either proarrhythmic or antiarrhythmic, depending on the mechanisms of arrhythmia.[5] While I_{KAS} may be important in cardiac arrhythmogenesis, whether I_{KAS} is present in the PCs remain unknown. The purpose of the present study is to test the hypotheses that there is a robust expression of SK proteins in the PCs, and that apamin significantly prolongs the APD of PCs isolated from normal rabbit ventricles.

Methods

This research protocol was approved by the Institutional Animal Care and Use Committee of Indiana University and the Methodist Research Institute, and was conducted in compliance with the Guide for the Care and Use of Laboratory Animals.[16] We studied 25 normal rabbit ventricles, including 13 patch-clamp studies, 4 for Western blotting, and 8 for immunohistochemical staining.

Cell Isolation

The cell isolation protocol was modified from published methods.[17] The rabbits underwent isoflurane inhalation general anesthesia. The chests were opened through median sternotomy and the hearts harvested and quickly placed in ice-cold normal Tyrode's solution that contained (in mmol/L): NaCl, 140; KCl, 5.4; $MgCl_2$, 1.2; NaH_2PO_4, 0.33; $CaCl_2$, 1.8; glucose, 10; and HEPES, 5 (pH 7.4 with NaOH). The ascending aortas were cannulated. Using a Langendorff perfusion setup, the hearts were perfused for 5 minutes with normal Tyrode's solution that contained calcium, followed by Tyrode's solution without calcium for 5 minutes, and then with Worthington's collagenase type II (360 u/mg, 0.4 g/L) until the flow rate rapidly increased (15–20 minutes). Hearts were briefly flushed with Tyrode's solution without Ca and removed from

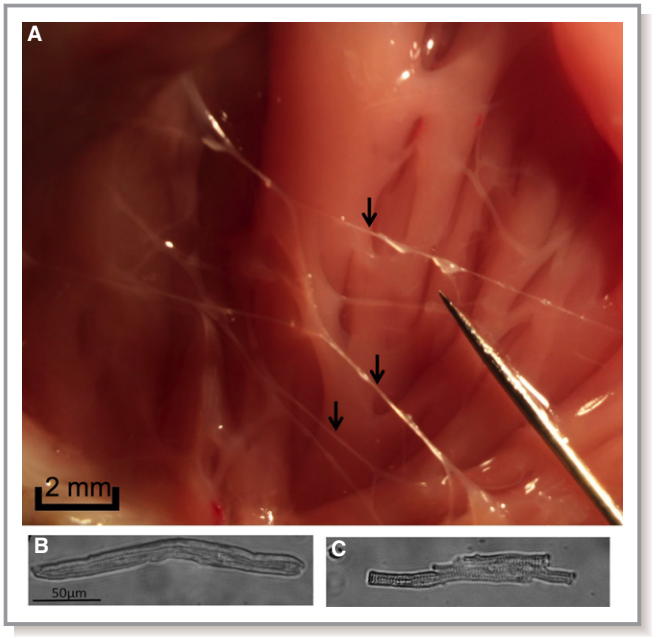

Figure 1. Cell isolation. A, Pseudotendons (arrows) within a normal rabbit left ventricle. Purkinje cells (PCs) were isolated from pseudotendons while myocytes were isolated from the myocardium. B, An isolated PC, which was identified by a tapered morphology at the end of the cell. C, An isolated ventricular myocyte, which has apparent transverse tubules and does not have a tapered end.

Langendorff setup. The ventricles were carefully cut open to avoid applying shear stress to the pseudotendons and myocardium (Figure 1A). Pseudotendons (5–10) per prep were excised and then placed in a 15-mL Falcon tube with 10 mL of the collagenase perfusate. Pseudotendons were digested an additional 20 minutes (until visibly digested) in a 37°C shaker. While pseudotendons were further digested, the VMs were gently shaken from the ventricle and placed in fresh normal Tyrode's solution. Pseudotendons were allowed to settle to the bottom of the Falcon tube after digestion. Supernatant was replaced with high K disaggregation solution, including (in mmol/L): L-glutamic acid (mono-K-salt), 145.7; $MgCl_2 \cdot 6H_2O$, 203.31; and HEPES, 5 (pH to 6.71–6.72 with KOH). Solution was gently triturated with Fisher Borosilicate Glass Pasteur pipettes (Thermo Fisher Scientific, Waltham, MA) until the solution became cloudy. Pseudotendons were allowed to settle and supernatant containing isolated PCs was transferred to a new tube and replaced with fresh disaggregation solution. Trituration was repeated several times. Isolated PCs were allowed to settle and the supernatant was changed to normal Tyrode's solution. Calcium was slowly titrated to 1.8 mmol/L for PCs and VMs. Cells were kept on ice until used (within 8 hours). Cells were also morphologically identified before patch to confirm that membranes were healthy, free of blebs or contractures, displaying visible striations, and that individual cells, rather than clusters, were

being patched. Figure 1B and 1C show a PC and a VM, respectively. As compared with VMs, the PCs were larger, less striated, and had tapered ends.

Patch-Clamp Studies

Current-clamp recordings were performed at 37°C, regulated by a PH-1 heating platform, SH-27B solution heater, and TC-344B temperature controller (Warner Instruments, Hamden, CT). Voltage-clamp experiments were conducted at room temperature (21–23°C). Axopatch 200B amplifier and pCLAMP-10 software (Axon; Molecular Devices, Sunnyvale, CA) were used to generate and record all patch experiments. Pipette electrodes were fabricated using Corning 7056 glass capillaries (Warner Instruments). The pipette resistance was 3 to 5 MΩ for all experiments in the bath solution. The perforated patch technique was used to record transmembrane action potentials (APs) in current-clamp mode Pipette solution contained (in mmol/L): K-glutamate, 120; KCl, 25; $MgCl_2$, 1; $CaCl_2$, 2; and HEPES, 10 (pH 7.4 with KOH); and back-filled with the same solution containing 200 μg/mL amphotericin B. Data were corrected for the calculated liquid junction potential (+14.3 mV). Extracellular Tyrode's solution containing 1.8 mmol/L $CaCl_2$ was used. PCs and VMs were kept separate throughout the disaggregation procedures. Action potentials were evoked by 2-ms current pulses ranging from 1 to 2 nA. APD measured to 80% repolarization (APD_{80}) at different PCLs was obtained at baseline and after adding 100 nmol/L of apamin to the superfusion solution.

For whole-cell I_{KAS} measurements, the pipette solution contained (in mmol/L): potassium gluconate, 144; EGTA, 5; HEPES, 10; 1 μmol/L free calcium (measured with perfectION combination calcium electrode); and pH 7.25 (adjusted with potassium hydroxide). The extracellular solution contained (in mmol/L): *N*-methyl-glucamine, 140; KCl, 2; $MgCl_2$, 1; HEPES, 10; and pH, 7.4 (adjusted with HCl). The voltage-clamp protocol consisted of 500-ms square pulses to voltages ranging from −100 to +40 mV delivered in 20-mV increments from a holding potential of −50 mV. The interpulse interval was 5 seconds. Pipette resistance ranged from 1 to 2 MΩ. Series resistance was electronically compensated by 70% to 80%. To obtain whole-cell I_{KAS}, currents recorded in the presence of 100 nmole/L apamin were digitally subtracted from those recorded in its absence. I_{KAS} amplitudes for each test potential were determined by averaging the current over the entire duration of the voltage pulse using Clampfit (Molecular Devices).

Western Blotting

Four normal rabbit ventricles were isolated and Langendorff perfused with Tyrode's solution for 5 minutes to reduce the number of endogenous antibodies in the blood vessels. The ventricles were then placed on ice and cut open. All pseudotendons were collected from the right and left ventricular cavities. Afterwards the left ventricular free wall was excised and the endocardium was removed and discarded to eliminate the subendocardial PCs. The remaining left ventricular free wall was divided into the epicardial portion and the midmyocardial portion for separate analyses. All samples were directly homogenized in 20 mmol/L MOPS with 1% SDS in the presence of protease inhibitors. Eighty micrograms of each sample was loaded on SDS-PAGE and transferred to a nitrocellulose membrane. The blot was probed with an anti-SK2 polyclonal antibody (1:500, Sigma) and monoclonal anti-SERCA antibody 2A7-A1. Antibody-binding protein bands were visualized by ^{125}I-protein A and quantified with a Bio-Rad Personal Fx phosphorimager (Hercules, CA). The mean of intensity values from 4 rabbits was used. The control sample was cultured human embryonic kidney 293 cells infected by adenovirus encoding human isoform of subtype 2 SK (SK2).

Immunofluorescence Staining and Confocal Microscopy

Adult normal rabbit hearts (n=8) were fixed in 4% formalin for 45 to 60 minutes, followed by storage in 70% alcohol for at least 48 hours. The samples were then processed routinely and embedded in paraffin. Tissue sections (5 μm in thickness) were deparaffinized and hydrated by multiple Xylene washes and ethanol washes, followed by water and PBS with Tween 20 wash. Myocytes were then permeabilized and blocked in PBS with 3% BSA and 0.2% Triton X-100. After blocking, the slides were incubated with the polyclonal anti-SK2 antibody (1:500, Sigma), followed by secondary antibodies (Dako) for light microscope examinations. Adobe Photoshop version CS6 was used to study the average luminosity, which represents the intensity, or luminance, of the selected area of interest in an image. We first selected 10 areas in the VM, excluding the nucleus, and then used the histogram tool to determine the mean luminosity of the selected areas. We then used the same exact area but in the pseudotendon to determine the luminosity there. The average luminosity of the 10 PCs and 10 VMs were used to estimate the strength of immunostaining of PCs and VMs or that ventricle. If the cells are strongly stained with the antibody, then the luminosity is reduced.

For confocal microscopy studies, the secondary antibody conjugated with fluorescent dyes (Alexa 488 by Invitrogen) was used. Confocal images were obtained through a ×40 lens of DMI6000 Adaptive Focus Automated Inverted Microscope, Leica TCS SP8 FSU (Argon Ion Laser) SPectral Confocal System with HyD Super Sensitivity Detection. Both negative and positive controls were used to ensure quality of the stain.

Statistical Analysis

APD_{80} was measured at the level of 80% repolarization of APD and mean APD_{80} was calculated for all available data points. Continuous variables were expressed as mean and 95% CI or mean±SEM. Paired *t* tests were used to compare APD_{80} before and after apamin treatment at different PCLs. A linear-mixed effects model was also used to fit the APD_{80} data with the cell type, PCL, apamin treatment, and the interaction between apamin treatment and cell type as discrete fixed effects and cells treated as random effects.[18] For voltage-clamp studies, I_{KAS} densities for each cell under different ≥0 V were first averaged, and 2-sample *t* test was used to compare the averaged I_{KAS} densities. Two-sample *t* tests were used to compare the differences of, luminosity and SK2 protein expression between PCs and VMs. Bonferroni correction was applied for *t* tests with multiple comparisons. A $P \leq 0.05$ was considered statistically significant.

Results

For all results reported below, n refers to the number of cells unless otherwise noted.

Current-Clamp Studies

A total of 9 PCs from 6 rabbit ventricles were successfully studied. In addition, we studied 3 VMs from an additional 3 rabbit ventricles to confirm a previous observation that apamin has little effect on APD in normal VMs.[19] Figure 1 shows the endocardial pseudotendon of a normal rabbit ventricle (Figure 1A), a PC (Figure 1B), and a VM (Figure 1C). A PC was identified by its tapered cell morphology and a lack of transverse tubules.[10] PCs and VMs were selected for patch studies. Figure 2 illustrates the effects of apamin (100 nmol/L) on APD_{80} at different PCLs in PCs. As shown in Figure 2A through 2C, the ΔAPD_{80} (differences of APD_{80} before and after apamin) increased with increasing PCL. Figure 2D illustrates the methods used to measure APD_{80} and the duration of pacing pulse. An online supplement shows that the stimulus artifacts at the same PCL were the same before and after the exposure to apamin.

Figure 3 shows examples of apamin (100 nmol/L) effects on VMs. Apamin has little or no effect on these normal VMs at 600 or 1000 ms PCLs, which was consistent with the results of previous studies.[8,15,19,20] Figure 4 shows data from all PCs (Figure 4A) and VMs (Figure 4B) studied. Each cell is coded with a unique color. The baseline APD_{80} is shown in unfilled

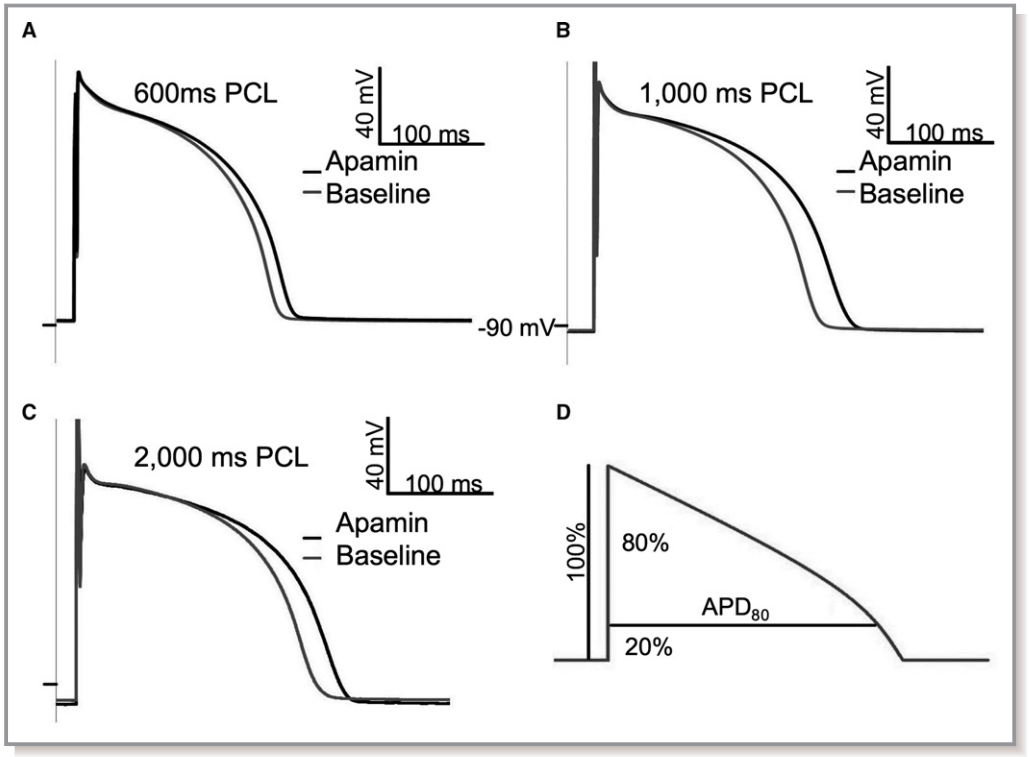

Figure 2. Effects of apamin on action potential duration measured to 80% repolarization (APD_{80}) of a Purkinje cell (PC) paced at different cycle lengths. A through C, The effects at 600, 1000, and 2000 ms pacing cycle length (PCL), respectively. Note a smaller change in APD_{80} with 600 ms PCL than with 1000 or 2000 ms PCLs. D, A schematic of how the APD_{80} was measured.

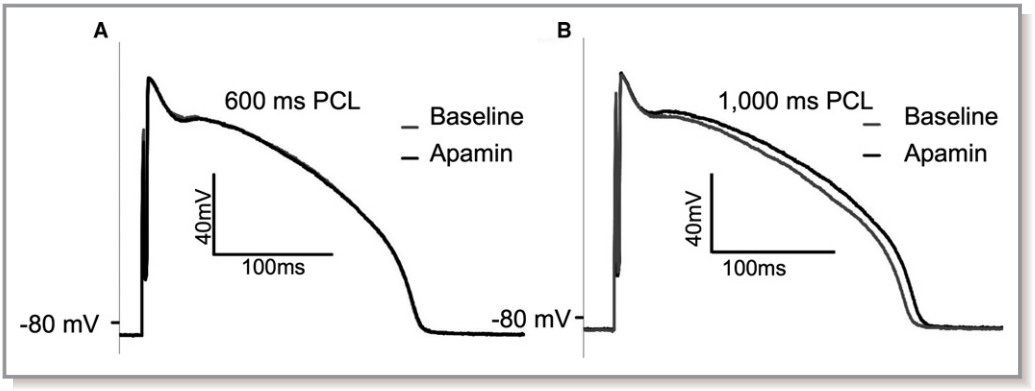

Figure 3. Effects of apamin on action potential duration measured to 80% repolarization (APD_{80}) of the ventricular myocytes at 600 ms pacing cycle length (PCL) (A) and 1000 ms PCL (B). Note the slight APD_{80} prolongation at 1000 ms PCL but not at 600 ms PCL.

circles while the APD_{80} after apamin is shown in filled circles. A line segment was used to connect the data from the same cell. Figure 4A shows that apamin prolonged APD_{80} in most but not all PCs at different PCLs. The magnitudes of prolongation (ΔAPD_{80}) of the PCs are shown in Figure 4C. Figure 4B shows the effects of apamin on APD_{80} of VMs at various PCLs. The ΔAPD_{80} of VMs are shown in Figure 4D. Apamin induced very little change of APD_{80} in VMs at PCLs between 500 and 1000 ms. APD_{80} prolongation was observed with 2000 and 4000 ms PCLs. The latter finding is consistent with a previous study which showed that apamin increased APD_{80} of Langendorff-perfused normal rabbit ventricles only when the PCL was ≥800 ms.[21] For all cells studied, apamin prolonged APD_{80} of PCs (n=9) from 228±12 to 244±17 ms (6.63% increase) at 2000 ms PCL, from 203±18 to 226±3 ms (9.22% increase) at 1000 ms PCL,

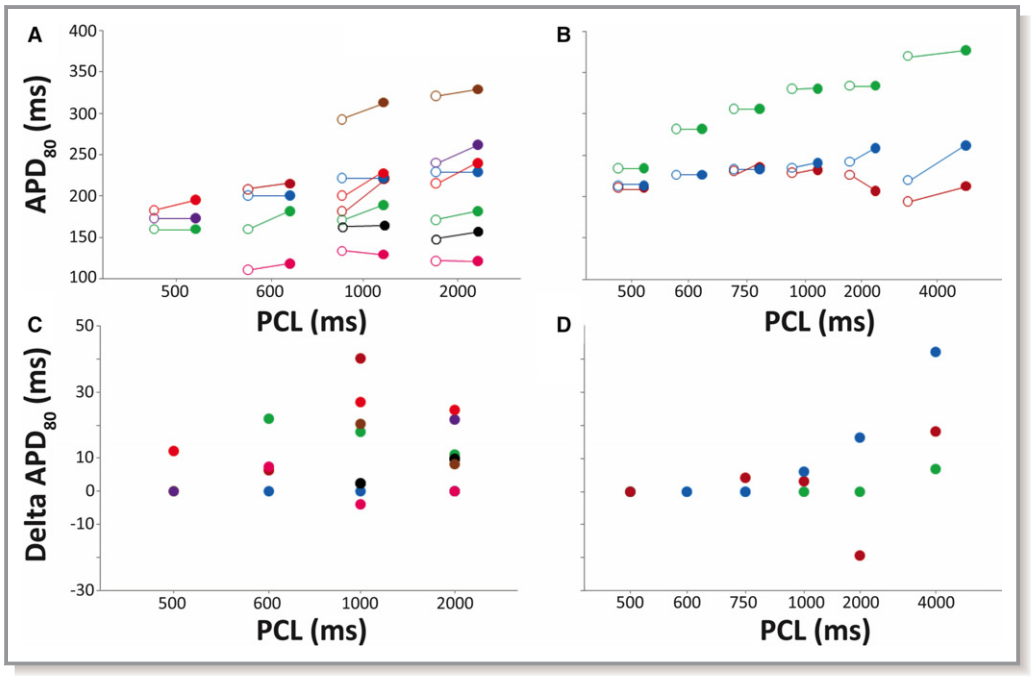

Figure 4. The relationship between action potential duration measured to 80% repolarization (APD_{80}) and pacing cycle length (PCL) of all cells studied. Each cell is coded with a unique color. The APD_{80} values at baseline are shown in unfilled circles while those after apamin are shown in filled circles. A short line segment connects the APD_{80} before and after apamin of each cell. Because each cell was paced at 2 to 3 different PCLs, there were 21 data pairs from 9 Purkinje cells (PCs) studied (A) and 16 data pairs from 3 ventricular myocytes (VMs) studied (B). C and D, Change (delta) in APD_{80} of the PCs and VMs, respectively. PCs may show APD_{80} prolongation after apamin administration at all PCLs. However, apamin did not change APD_{80} in VMs with PCL <1000 ms.

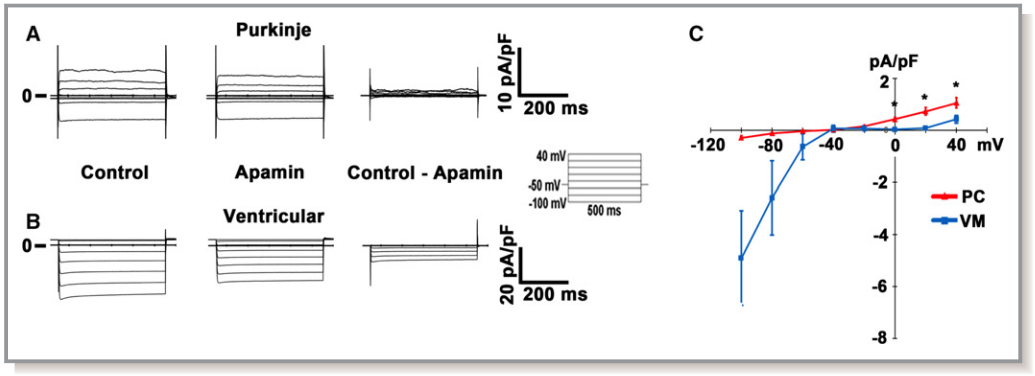

Figure 5. Patch-clamp studies. Representative whole-cell current recordings obtained from a Purkinje cell (PC) (A) and a ventricular myocyte (VM) (B) before and after 100 nmol/L apamin. The right panels show apamin-sensitive difference currents. Insert: voltage-clamp protocol. The capacitance of PCs was 82.86 (95% CI, 68.19–97.52) pF. The capacitance of VMs was 127.60 (95% CI, 92.12–163.0) pF. C, Plots of apamin-sensitive whole-cell current densities as a function of test potential. Values are mean±SEM from 6 cells per cell type. **P*<0.05 vs VM by *t* test.

from 190±26 to 199±16 ms (5.58% increase) at 600 ms PCL and from 171±16 to 177±25 ms (2.2% increase) at 500 ms PCL. The range of ΔAPD_{80} was 0 to 24 ms at 2000 ms PCL, 0 to 41 ms at 1000 ms PLC, 0 to 22 ms at 600 ms PCL, and 0 to 12 ms at 500 ms PCL. In comparison, APD_{80} of VMs did not change at 500 or 600 ms PCL but changed by 0 to 4 ms at 750 ms PCL, 0 to 3 ms at 1000 ms PCL, −19 to 16 ms at 2000 ms PCL, and 7 to 42 ms at 4000 ms PCL. A linear-mixed effects model was used to fit the APD_{80} data with cells treated as random effects. For PCs, the apamin significantly prolonged APD_{80} by an average of 10.4 ms (95% CI, 0.11–20.72) (n=9, *P*=0.047). For VMs, the apamin insignificantly prolonged APD_{80} by an average of 4.58 ms (95% CI, −7.18 to 16.34) (n=3, *P*=0.45).

Voltage-Clamp Studies

Representative recordings of whole-cell currents from a PC and a VM in the absence and presence of 100 nmole/L apamin are shown in Figure 5A and 5B. There are 6 cells from each of the PC and VM groups (a total of 12 cells). For each cell, the I_{KAS} density was measured under 8 different voltage levels. I_{KAS} densities for each cell were averaged over the 3 positive voltage levels. A 2-sample *t* test was then used to compare the averaged I_{KAS} densities between the PC and VM groups. Results from Shapiro–Wilk normality test were not significant for either group (*P*=0.79 for PCs and *P*=0.71 for VM). Mean I_{KAS} density was significantly larger in PC cells compared with VMs at potentials ≥0 mV (Figure 5C; *P*<0.05).

SK2 Protein Expression in the Pseudotendon

We performed quantitative Western blot analyses to compare the expression level of SK2 protein between pseudotendon, epicardium, and midmyocardium. As shown in Figure 6, expression of SK2 protein in pseudotendon was confirmed as a protein band with a molecular mass of about 60 kDa. The SK2 expression in the midmyocardium was 58% (95% CI, 25–91) (n=4, *P*=0.028) of that in the pseudotendon. The SK2 protein expression in the epicardium was 50% (95% CI, 16–83) (n=4, *P*=0.018) of that in the pseudotendon. These findings

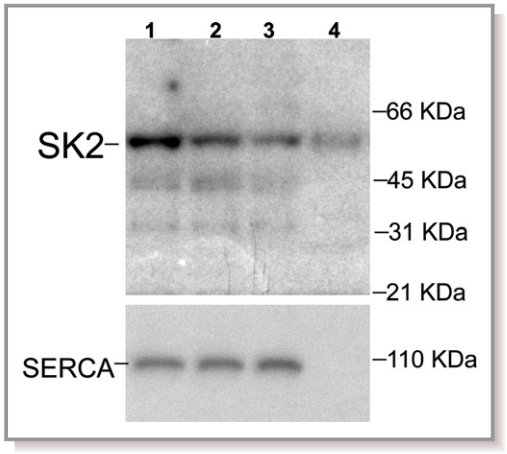

Figure 6. Western blot analysis of small-conductance calcium-activated potassium subtype 2 (SK2) protein expression. Each lane contained 80 µg homogenates of pseudotendon, epicardium, and midmyocardium. The control sample was human embryonic kidney cells infected by adenovirus encoding human isoform of SK2. The blot was probed with an anti-SK2 polyclonal antibody (1:500, Sigma). Antibody-binding protein bands were visualized by ^{125}I-protein A and quantified with a Bio-Rad Personal Fx phosphorimager. These data show that SK2 protein expression is higher in pseutotendon than myocardium.

indicate that there is greater expression of SK2 protein in pseudotendon than in midmyocardium and epicardium.

Immunohistochemical Studies

Consistent with our Western blot analyses, immunohistochemical studies of the rabbit ventricles showed stronger staining of SK2 proteins in PCs than in VMs. These findings were consistent in all 8 normal rabbit ventricles studied. Figure 7A shows a cross-section of pseudotendon (arrow) and the neighboring ventricular myocardium. The brown color indicates positive staining. The staining is much stronger in the PCs within the pseudotendon than that of the VMs in the neighboring ventricular tissues. Figure 7B shows a picture from a different ventricle. The endocardial PCs (arrow) stained much stronger than the surrounding VMs. We used Photoshop to determine the luminosity of the PCs and VMs in all 8 ventricles. The luminosity of VMs was 91 in the 8 ventricles (95% CI, 78–104), significantly (P=0.0088) higher than that of the PCs (67; 95% CI, 54–81). The latter finding indicates that PCs were stained stronger with the antibody than VMs, thus reducing the light going through the cell. Figure 7C shows immunofluorescent staining of the PCs in the pseudotendon, showing strong staining at the periphery of the PCs. Figure 7D shows immunofluorescent staining of a PC at the endocardium. The PC (arrow) stained stronger than the surrounding VMs. The peripheral distribution of the SK2 protein was consistently observed in all ventricles examined.

Discussion

The primary findings of this study are that: (1) there was greater expression of SK protein and I_{KAS} in PCs than VMs; and (2) apamin prolonged the APD_{80} in PCs isolated from

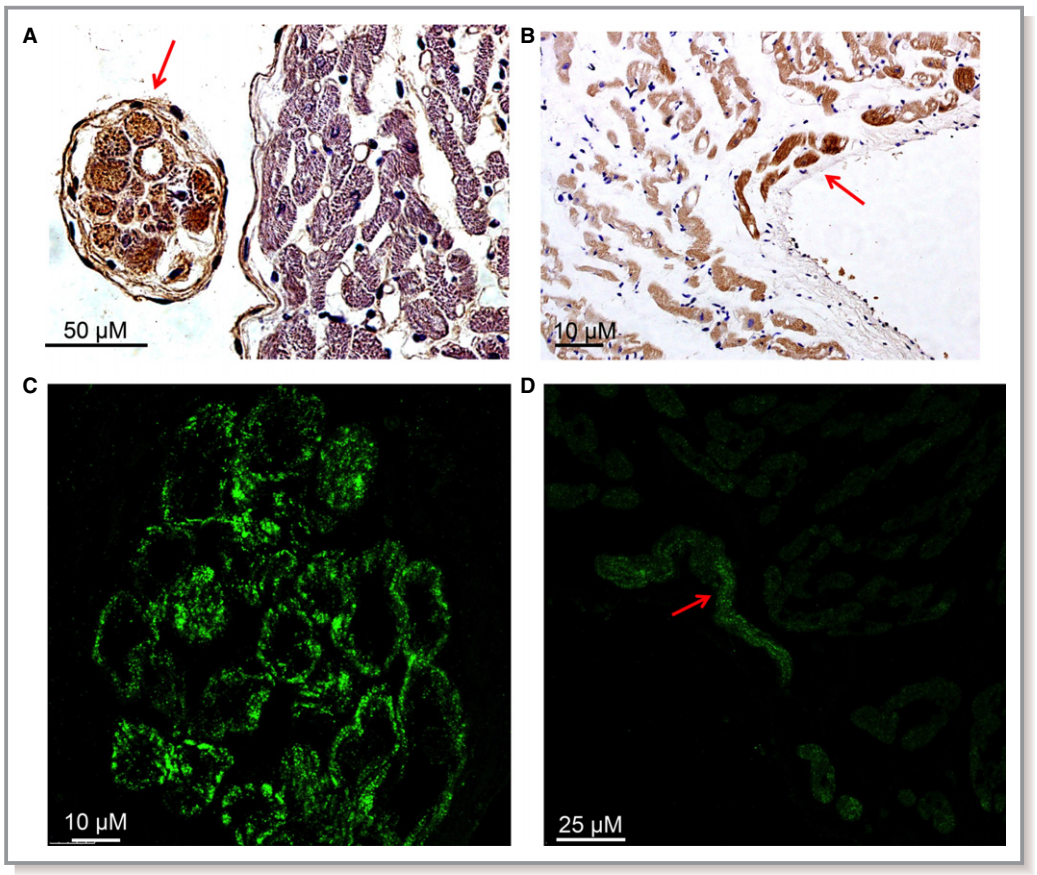

Figure 7. Immunohistochemical studies of normal rabbit ventricles stained for small-conductance calcium-activated potassium subtype 2 protein. A and B, Light microscopic findings. A, A pseudotendon (arrow) and neighboring myocardium. The Purkinje cells (PCs) in the pseudotendon stained strongly positive (brown) while the neighboring myocardium was only lightly stained (peroxidase stain ×400). B, Endocardial PCs in a different ventricle (arrow) stained much stronger than the adjacent myocardium (peroxidase stain ×100). C and D, Confocal microscopic images of ventricles stained with immunofluorescent secondary antibodies. C, The cross-section of a pseudotendon. The confocal optical section showed that almost all PCs have primarily peripheral staining (×400). D, A strongly stained PC (arrow).

normal rabbit ventricles at all PCLs, but prolonged APD_{80} of VMs only at long PCLs. The effects of apamin on APD_{80} are not uniform, suggesting a highly variable amount of I_{KAS} among different PCs and VMs. These findings indicate that SK channel proteins are more abundantly present in normal rabbit PCs than VMs, and that I_{KAS} is more important in normal PC repolarization than in VM repolarization at normal or nearly normal activation rates.

Distinct Electrophysiological Characteristics of PCs

Gorza et al[22] found that conduction tissue cells of the rabbit heart originate from a population of neural crest–derived cells migrating from the branchial arches into the developing heart. These conduction cells have been found to express proteins and epitopes common with those in neural tissue.[23] Because SK proteins are abundantly present in the neuronal tissues,[1] this lineage may partially explain the differential SK current densities between the PCs and VMs. However, others showed that cardiac PCs and working myocytes share a common myogenic precursor and that migratory neuroectoderm-derived populations do not contribute to the development of PCs.[24,25] While there is no consensus on the neuronal origin of the PCs, there is little doubt that the PCs are electrophysiologically different than the working VMs.[10] Compared with VMs, the PCs have much smaller inward rectifier K+ current and much larger Ca^{2+}-independent transient outward K^+ current.[26] The differences in the densities of these potassium currents in part account for the differences of the electrophysiological properties between PCs and VMs. A reduced inward rectifier K+ current can increase the diastolic Ca^{2+}-membrane potential coupling gain and facilitate the development of afterdepolarization and triggered activity from PCs in intact rabbit ventricles.[11] PCs had greater expression of minK-related peptide 1, the product of the potassium voltage-gated channel subfamily E member 2 gene, than the VMs.[27] These changes make PC a strong candidate to play a role in arrhythmic syndromes due to minK-related peptide 1 abnormalities, such as long QT syndrome and ventricular fibrillation.[28] While both PCs and VMs contain pacemaker (funny) current, only in PCs did the current activate in the physiological range.[29] Callewaert et al[30] previously reported the existence of calcium-dependent potassium channels in the membrane of cow cardiac PCs. However, because that study was performed prior to the cloning of the SK channels, there was no immunohistochemical or Western blotting data on the existence of SK proteins in the cow cardiac PCs. The present study extends that observation by documenting a difference of I_{KAS} between PCs and VMs, and by demonstrating a more abundant presence of SK2 proteins in the PCs than in the VMs. These results suggest that I_{KAS} plays an important role in the repolarization of PCs, and may in part account for the differential electrophysiological characteristics of the PCs and VMs.

Importance of Activation Rates

Heart rate is known to play an important role in regulating the I_{KAS} in failing ventricles. An extremely high rate of activation, such as that which occurs during ventricular fibrillation, is known to activate I_{KAS} and shorten the postshock APD. These changes facilitate the recurrence of ventricular fibrillation in failing rabbit ventricles.[15,31] Hsieh et al[7] tested the importance of pacing rates on the expression of I_{KAS} in the same rabbit heart failure model. The results show that apamin lengthens the APD of the epicardium at either very short or very long PCLs, but not at intermediate PCLs. In the present study, we found similar results in nonfailing PCs. We were not able to pace at <500 ms in isolated PCs. However, when the PCL was increased, the effects of apamin on APD also increased significantly. In addition, the apamin was able to prolong APD of the VMs at long but not short PCLs. The mechanism by which slow pacing rate facilitated the upregulation of I_{KAS} might be due to increased intracellular calcium at slow pacing rates.[32,33] An additional factor might be related to the longer duration of L-type Ca^{2+} current activation when APD is prolonged. Because the SK channel is coupled to L-type Ca^{2+} channels via alpha-actinin 2,[34] prolonged activation of L-type Ca^{2+} current may prolong the opening of the SK channels. These findings also suggest that inadvertent blockade of I_{KAS} by food or drugs might reduce repolarization reserve and promote ventricular arrhythmias when the heart rate is slow, such as during atrioventricular block.[21]

Limitations

There were large variations of apamin responses among different PCs. Large variations of I_{KAS} densities have also been observed in VMs.[8,15,35] The mechanisms by which some cells had more I_{KAS} than others remain unclear.

Conclusions

These data indicate that SK2 proteins are more abundantly present in the PCs than in VMs of normal rabbit ventricles. I_{KAS} is important in ventricular repolarization of normal PCs.

Acknowledgments

We thank Nicole Courtney, Jessica Warfel, and Glen Schmeisser for their assistance.

Sources of Funding

This study was supported in part by National Institutes of Health/National Heart, Lung, and Blood Institute grants P01HL78931, R01HL71140, and R41HL124741; a Medtronic-Zipes Endowment (P.-S. Chen); the Indiana University Health-Indiana University School of Medicine Strategic Research Initiative; and National Institutes of Health R01HL105983 (Boyden). The content is solely the responsibility of the authors and does not necessarily represent the official views of the National Institutes of Health.

Disclosures

None.

References

1. Kohler M, Hirschberg B, Bond CT, Kinzie JM, Marrion NV, Maylie J, Adelman JP. Small-conductance, calcium-activated potassium channels from mammalian brain. *Science*. 1996;273:1709–1714.
2. Adelman JP, Maylie J, Sah P. Small-conductance Ca(2+)-activated K(+) channels: form and function. *Annu Rev Physiol*. 2012;74:245–269.
3. Yu CC, Ai T, Weiss JN, Chen PS. Apamin does not inhibit human cardiac Na^+ current, L-type Ca^{2+} current or other major K^+ currents. *PLoS One*. 2014;9:e96691.
4. Grillner S. The motor infrastructure: from ion channels to neuronal networks. *Nat Rev Neurosci*. 2003;4:573–586.
5. Chang PC, Chen PS. SK channels and ventricular arrhythmias in heart failure. *Trends Cardiovasc Med*. 2015;25:508–514.
6. Zhang XD, Lieu DK, Chiamvimonvat N. Small-conductance Ca^{2+}-activated K^+ channels and cardiac arrhythmias. *Heart Rhythm*. 2015;12:1845–1851.
7. Hsieh YC, Chang PC, Hsueh CH, Lee YS, Shen C, Weiss JN, Chen Z, Ai T, Lin SF, Chen PS. Apamin-sensitive potassium current modulates action potential duration restitution and arrhythmogenesis of failing rabbit ventricles. *Circ Arrhythm Electrophysiol*. 2013;6:410–418.
8. Chang PC, Turker I, Lopshire JC, Masroor S, Nguyen BL, Tao W, Rubart M, Chen PS, Chen Z, Ai T. Heterogeneous upregulation of apamin-sensitive potassium currents in failing human ventricles. *J Am Heart Assoc*. 2013;2:e004713. DOI: 10.1161/JAHA.112.004713.
9. Ideker RE, Kong W, Pogwizd S. Purkinje fibers and arrhythmias. *Pacing Clin Electrophysiol*. 2009;32:283–285.
10. Boyden PA, Dun W, Robinson RB. Cardiac Purkinje fibers and arrhythmias; The GK Moe Award Lecture 2015. *Heart Rhythm*. 2016;13:1172–1181.
11. Maruyama M, Joung B, Tang L, Shinohara T, On YK, Han S, Choi EK, Kim DH, Shen MJ, Weiss JN, Lin SF, Chen PS. Diastolic intracellular calcium-membrane voltage coupling gain and postshock arrhythmias: role of Purkinje fibers and triggered activity. *Circ Res*. 2010;106:399–408.
12. Tabereaux PB, Walcott GP, Rogers JM, Kim J, Dosdall DJ, Robertson PG, Killingsworth CR, Smith WM, Ideker RE. Activation patterns of Purkinje fibers during long-duration ventricular fibrillation in an isolated canine heart model. *Circulation*. 2007;116:1113–1119.
13. Haissaguerre M, Extramiana F, Hocini M, Cauchemez B, Jais P, Cabrera JA, Farre G, Leenhardt A, Sanders P, Scavee C, Hsu LF, Weerasooriya R, Shah DC, Frank R, Maury P, Delay M, Garrigue S, Clementy J. Mapping and ablation of ventricular fibrillation associated with long-QT and Brugada syndromes. *Circulation*. 2003;108:925–928.
14. Boyden PA, Barbhaiya C, Lee T, ter Keurs HE. Nonuniform Ca^{2+} transients in arrhythmogenic Purkinje cells that survive in the infarcted canine heart. *Cardiovasc Res*. 2003;57:681–693.
15. Chua SK, Chang PC, Maruyama M, Turker I, Shinohara T, Shen MJ, Chen Z, Shen C, Rubart-von der Lohe M, Lopshire JC, Ogawa M, Weiss JN, Lin SF, Ai T, Chen PS. Small-conductance calcium-activated potassium channel and recurrent ventricular fibrillation in failing rabbit ventricles. *Circ Res*. 2011;108:971–979.
16. National Research Council. *Guide for the Care and Use of Laboratory Animals*. 8th ed. Washington, DC: National Academies Press (US); 2011.
17. Boyden PA, Albala A, Dresdner KP Jr. Electrophysiology and ultrastructure of canine subendocardial Purkinje cells isolated from control and 24-hour infarcted hearts. *Circ Res*. 1989;65:955–970.
18. Laird NM, Ware JH. Random-effects models for longitudinal data. *Biometrics*. 1982;38:963–974.
19. Nagy N, Szuts V, Horvath Z, Seprenyi G, Farkas AS, Acsai K, Prorok J, Bitay M, Kun A, Pataricza J, Papp JG, Nanasi PP, Varro A, Toth A. Does small-conductance calcium-activated potassium channel contribute to cardiac repolarization? *J Mol Cell Cardiol*. 2009;47:656–663.
20. Lee YS, Chang PC, Hsueh CH, Maruyama M, Park HW, Rhee KS, Hsieh YC, Shen C, Weiss JN, Chen Z, Lin SF, Chen PS. Apamin-sensitive calcium-activated potassium currents in rabbit ventricles with chronic myocardial infarction. *J Cardiovasc Electrophysiol*. 2013;24:1144–1153.
21. Chang PC, Hsieh YC, Hsueh CH, Weiss JN, Lin SF, Chen PS. Apamin induces early afterdepolarizations and Torsades de Pointes ventricular arrhythmia from failing rabbit ventricles exhibiting secondary rises in intracellular calcium. *Heart Rhythm*. 2013;10:1516–1524.
22. Gorza L, Schiaffino S, Vitadello M. Heart conduction system: a neural crest derivative? *Brain Res*. 1988;457:360–366.
23. Gorza L, Vettore S, Vitadello M. Molecular and cellular diversity of heart conduction system myocytes. *Trends Cardiovasc Med*. 1994;4:153–159.
24. Gourdie RG, Mima T, Thompson RP, Mikawa T. Terminal diversification of the myocyte lineage generates Purkinje fibers of the cardiac conduction system. *Development*. 1995;121:1423–1431.
25. Cheng G, Litchenberg WH, Cole GJ, Mikawa T, Thompson RP, Gourdie RG. Development of the cardiac conduction system involves recruitment within a multipotent cardiomyogenic lineage. *Development*. 1999;126:5041–5049.
26. Cordeiro JM, Spitzer KW, Giles WR. Repolarizing K+ currents in rabbit heart Purkinje cells. *J Physiol*. 1998;508(pt 3):811–823.
27. Pourrier M, Zicha S, Ehrlich J, Han W, Nattel S. Canine ventricular KCNE2 expression resides predominantly in Purkinje fibers. *Circ Res*. 2003;93:189–191.
28. Abbott GW, Sesti F, Splawski I, Buck ME, Lehmann MH, Timothy KW, Keating MT, Goldstein SA. MiRP1 forms IKr potassium channels with HERG and is associated with cardiac arrhythmia. *Cell*. 1999;97:175–187.
29. Yu H, Chang F, Cohen IS. Pacemaker current i(f) in adult canine cardiac ventricular myocytes. *J Physiol*. 1995;485(pt 2):469–483.
30. Callewaert G, Vereecke J, Carmeliet E. Existence of a calcium-dependent potassium channel in the membrane of cow cardiac Purkinje cells. *Pflugers Arch*. 1986;406:424–426.
31. Ogawa M, Morita N, Tang L, Karagueuzian HS, Weiss JN, Lin SF, Chen PS. Mechanisms of recurrent ventricular fibrillation in a rabbit model of pacing-induced heart failure. *Heart Rhythm*. 2009;6:784–792.
32. Hasenfuss G, Pieske B. Calcium cycling in congestive heart failure. *J Mol Cell Cardiol*. 2002;34:951–969.
33. Schillinger W, Teucher N, Christians C, Kohlhaas M, Sossalla S, Van Nguyen P, Schmidt AG, Schunck O, Nebendahl K, Maier LS, Zeitz O, Hasenfuss G. High intracellular Na+ preserves myocardial function at low heart rates in isolated myocardium from failing hearts. *Eur J Heart Fail*. 2006;8:673–680.
34. Lu L, Zhang Q, Timofeyev V, Zhang Z, Young JN, Shin HS, Knowlton AA, Chiamvimonvat N. Molecular coupling of a Ca^{2+}-activated K^+ channel to L-type Ca^{2+} channels via alpha-actinin2. *Circ Res*. 2007;100:112–120.
35. Yu CC, Corr C, Shen C, Shelton R, Yadava M, Rhea I, Straka S, Fishbein MC, Chen Z, Lin SF, Lopshire JC, Chen PS. Small conductance calcium-activated potassium current is important in transmural repolarization of failing human ventricles. *Circ Arrhythm Electrophysiol*. 2015;8:667–676.